



# Formation of magnetite-enriched zones in and offshore of a mesotidal estuarine lagoon: An environmental magnetic study of Tauranga Harbour and Bay of Plenty, New Zealand

## Firoz Badesab

*MARUM-Center for Marine Environmental Sciences and Faculty of Geosciences, University of Bremen, Klagenfurter Strasse, DE-28359 Bremen, Germany (firoz@uni-bremen.de)*

*Department of Earth and Ocean Sciences, University of Waikato, Private Bag 3105, Hamilton, New Zealand*

## Tilo von Dobeneck

*MARUM-Center for Marine Environmental Sciences and Faculty of Geosciences, University of Bremen, Klagenfurter Strasse, DE-28359 Bremen, Germany*

## Karin R. Bryan

*Department of Earth and Ocean Sciences, University of Waikato, Private Bag 3105, Hamilton, New Zealand*

## Hendrik Müller

*MARUM-Center for Marine Environmental Sciences and Faculty of Geosciences, University of Bremen, Klagenfurter Strasse, DE-28359 Bremen, Germany*

## Roger M. Briggs

*Department of Earth and Ocean Sciences, University of Waikato, Private Bag 3105, Hamilton, New Zealand*

## Thomas Frederichs and Eva Kwohl

*MARUM-Center for Marine Environmental Sciences and Faculty of Geosciences, University of Bremen, Klagenfurter Strasse, DE-28359 Bremen, Germany*

[1] Magnetic iron minerals are widespread and indicative sediment constituents in estuarine, coastal and shelf systems. We combine environmental magnetic, sedimentological and numerical methods to identify magnetite-enriched placer-like zones in a complex coastal system and delineate their formation mechanisms. Magnetic susceptibility and remanence measurements on 245 surficial sediment samples collected in and around Tauranga Harbour, the largest barrier-enclosed tidal estuary of New Zealand, reveal several discrete enrichment zones controlled by local hydrodynamic conditions. Active magnetite enrichment takes place in tidal channels, which feed into two coast-parallel nearshore magnetite-enriched belts centered at water depths of 6–10 m and 10–20 m. A close correlation between magnetite content and magnetic grain size was found, where higher susceptibility values are associated within coarser magnetic crystal sizes. Two key mechanisms for magnetite enrichment are identified. First, tide-induced residual currents primarily enable magnetite enrichment within the estuarine channel network. A coast-parallel, fine sand magnetite enrichment belt in water depths of less than 10 m along the barrier island has a strong decrease in magnetite

content away from the southern tidal inlet and is apparently related to active coast-parallel transport combined with mobilizing surf zone processes. A second, less pronounced, but more uniform magnetite enrichment belt at 10–20 m water depth is composed of non-mobile, medium-coarse-grained relict sands, which have been reworked during post-glacial sea level transgression. We demonstrate the potential of magnetic methods to reveal and differentiate coastal magnetite enrichment patterns and investigate their formative mechanisms.

**Components:** 9800 words, 9 figures, 1 table.

**Keywords:** environmental magnetism; magnetite enrichment; placer deposit; residual currents.

**Index Terms:** 1512 Geomagnetism and Paleomagnetism: Environmental magnetism; 4217 Oceanography: General: Coastal processes; 4534 Oceanography: Physical: Hydrodynamic modeling.

**Received** 27 February 2012; **Revised** 7 May 2012; **Accepted** 14 May 2012; **Published** 16 June 2012.

Badesab, F., T. von Dobeneck, K. R. Bryan, H. Müller, R. M. Briggs, T. Frederichs, and E. Kwohl (2012), Formation of magnetite-enriched zones in and offshore of a mesotidal estuarine lagoon: An environmental magnetic study of Tauranga Harbour and Bay of Plenty, New Zealand, *Geochem. Geophys. Geosyst.*, 13, Q06012, doi:10.1029/2012GC004125.

## 1. Introduction

[2] Heavy mineral enrichments known as ‘placers’ are found along many of the world’s coasts, with the economically most significant deposits being in Alaska (gold), India (magnetite), New Zealand (titanomagnetite) and Australia (rutile, monazite and zircon) [Rao, 1957; Gow, 1967; Komar and Wang, 1984; Li and Komar, 1992]. These enrichments are formed by physical concentration of detrital heavy mineral particles by action of winds, waves and currents mainly owing to their much greater density, but occasionally also supported by greater wear and weathering resistance. The concentration of detrital heavy mineral grains in fluvial estuaries and beaches is mostly explained by selective entrainment and dispersal of hydraulically equivalent particles of lesser densities and therefore large sizes [Slingerland, 1977]. Rapid burial of denser mineral particles due to gravitational effects may be an essential further enhancement process, which has been accounted for swash zone magnetite enrichment [Gallaway *et al.*, 2012]. Numerous investigations [Rao, 1957; Komar and Wang, 1984; Frihy and Dewidar, 2003] highlight the role of wave-induced currents, selective entrainment and gravitational sorting processes in concentrating heavy minerals especially on open coast beaches. Precise knowledge of the location, shape and composition of enrichment structures can also provide clues about past and present hydrodynamic conditions.

[3] Titanomagnetite is a common iron-titanium oxide mineral, which occurs as an accessory in both igneous and metamorphic rocks. Because of its widespread occurrence and high specific density, it is frequently concentrated in placer deposits and is often associated with other heavy minerals of higher economic value. Such ‘ironsand’ or ‘black sand’ placer deposits are particularly prevalent on the open west coast of the North Island of New Zealand [Carter, 1980; Bryan *et al.*, 2007], and form an economically important resource for New Zealand’s titanium and iron ore industry. Previous studies have shown that andesitic rocks from Mt Taranaki are the primary source of this black sand and that the northerly directed littoral drift system plays a key role in accumulation and distribution of these deposits along the west coast [Kear, 1979; Hamill and Ballance, 1985]. Bryan *et al.* [2007] investigated the spatial and temporal variability of titanomagnetite placers on west coast beaches using hydrodynamic modeling and mineralogical analyses. However, few attempts have been made to investigate New Zealand’s more sheltered, deeply embayed and partly lagoonal northeast coast for heavy mineral enrichments, largely because of the generally much lower and hence economically irrelevant titanomagnetite and ilmenite contents.

[4] Embayed, estuarine and lagoonal coastal environments are hydrodynamically more complex settings with wave and current intensities that vary widely over short distances due to changing fetch and morphological constrictions such as tidal channel networks. A better understanding of heavy

mineral concentration processes in such systems can help not only to detect localized enrichments but also to reveal unknown aspects and details of the underlying hydro- and sediment dynamics. Several factors can determine the morphology and evolution of barrier-enclosed estuaries, including sea level rise, sediment sources, river runoff, tidal exchange and hydrodynamics of the nearshore region [Komar, 1998]. Tide-induced residual currents contribute greatly to mass sediment transport. Such currents are generated by nonlinear interaction of tidal flow with variable bathymetry [Zimmerman, 1981], which produces changes in flood-ebb asymmetries and long-term transport of sediment. Conversely, on open coasts, wave-induced littoral drift systems play a dominant role in transportation and distribution of sediments. Rates of net littoral drift can vary progressively along the coast, which results in a non-uniform distribution of sediments.

[5] In this study, we set out to investigate how tidal exchange, nearshore hydrodynamics and sea level change determine the patterns of heavy mineral enrichment in the meso-tidal estuarine lagoon of Tauranga Harbour and in the nearshore Bay of Plenty on the northeast coast of New Zealand. This economically active and ecologically sensitive region has recently gained world-wide attention with the wreck and oil and debris spills of the container ship MV *RENA* on 5 October 2011. From the viewpoint of sediment petrology, fluvial influx of magnetite from the Taupo Volcanic Zone through the lagoon contrasts with a comparably low background magnetite concentration of modern shelf sediments, which makes this study area ideal to investigate formative mechanisms of heavy mineral enrichment in sheltered, mesotidal, transitional coastal environments. Here, we focus on the ferrimagnetic heavy mineral (titano-)magnetite, which can be easily quantified and characterized by rock magnetic (laboratory) and electromagnetic (in situ) methods.

[6] Magnetic mineral concentrations and grain sizes can be derived from standard rock magnetic parameters [Thompson and Oldfield, 1986; Maher et al., 1999]. This so-called environmental magnetic approach has been used to investigate sediment sources and transport pathways, and to assess heavy metal pollution in coastal systems [Oldfield et al., 1985; Foster et al., 1991; Razjigaeva and Naumova, 1992; Oldfield and Yu, 1994; Lees and Pethick, 1995; Wheeler et al., 1999; Zhang et al., 2001; Hatfield and Maher, 2008, 2009]. The

method has also been used to map the spatial distribution and composition of magnetic minerals in the coastal zone, to assess their degree of sorting, and to identify areas of sediment accumulation and erosion [Cioppa et al., 2010; Hatfield et al., 2010; Zhang et al., 2010]. The technical ability to resolve magnetite distribution patterns in detail has been improved by the development of benthic electromagnetic profiling, which permits rapid mapping of magnetic susceptibility together with electrical conductivity [Müller et al., 2011, 2012]. This sample-based study is aimed at deepening fundamental understanding of geological and hydrodynamic processes as a prerequisite for future high-resolution mapping and modeling.

## 2. Study Area

### 2.1. Geography and Geology

[7] The Bay of Plenty region extends across a tectonically and volcanically active region of the North Island of New Zealand. Erosion can be intense and severe rain storms can generate and transport sediments to the coast resulting in rapid changes in the coastal zone. Most of the sediments reaching the Bay of Plenty are derived from proximal source rocks from the Taupo and Coromandel volcanic zones (Figure 1b), and have been extensively reworked during Holocene post-glacial sea level transgression [Beanland and Berryman, 1992].

[8] Tauranga Harbour is a large mesotidal estuarine lagoon situated centrally within the Bay of Plenty covering an area of 851 km<sup>2</sup> [Krüger and Healy, 2006]. It is enclosed by two Holocene tombolos and a 24-km-long sand barrier island, Matakana Island. Two tidal inlets, the natural Katikati entrance at the northern and the artificially deepened Tauranga entrance at the southern end, connect the lagoon with the bay area (Figure 1a). The seaward side of Matakana Island consists of shore-parallel relict foredunes, transgressive dunes and extensive back barrier deposits. The landward side of the island is covered by a mantle of tephra and other volcanic deposits [Shepherd et al., 2000]. Coastal sand barriers in New Zealand developed during the late Pleistocene and Holocene. Changes in sea level influenced the sediment flows and played a key role in barrier development [Shepherd and Hesp, 2003].

[9] The southern part of Tauranga Harbour is New Zealand's largest natural harbor and the country's biggest export port. The entrance has a mean tidal

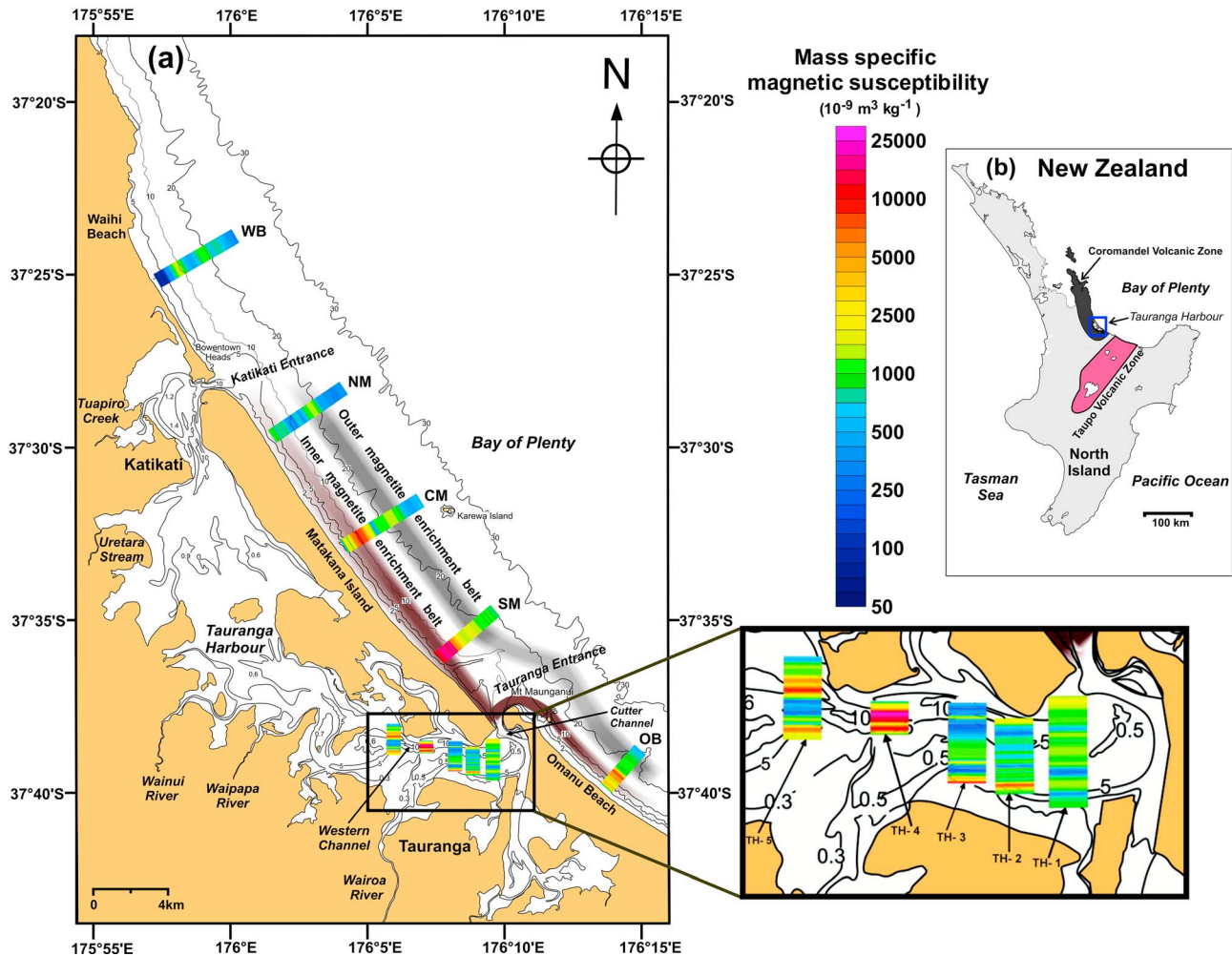


**Figure 1.** (a) Spatial distribution of magnetic minerals as indicated by concentration dependent magnetic susceptibility along the Bay of Plenty coast, New Zealand. TH-1, TH-2, TH-3, TH-4 represent the N-S oriented sediment sampling profiles within the southern basin of Tauranga Harbour. Five cross-shore profiles were named after Waihi Beach (WB), Northern Matakana (NM), Central Matakana (CM), Southern Matakana (SM) and Omanu Beach (OB). (b) Location map of the study area. This region is bounded by two major volcanic zones, the Coromandel Volcanic zone (CVZ) on the northwest and Taupo Volcanic zone (TVZ) on the southeast. Two hypothesized coast-parallel magnetite enrichment belts are highlighted using color gradients. The inner magnetite enrichment belt is indicated by dark brown and the outer belt is indicated with gray shading.

range of 1.4 m and a mean annual significant wave height of 0.5 m [De Lange, 1991]. The width of the entrance throat is 500 m with a maximum water depth of 34 m and a mean depth of 15 m [Krüger and Healy, 2006]. Wairoa River is the major fresh water source into Tauranga Harbour and has a large, mostly volcanic catchment area of about 465 km<sup>2</sup>. It contributes a sediment load of about 28,000 tonnes per year to the southern part of Tauranga Harbour which is approximately 42% of the total received load. Present-day sedimentation within the southern Tauranga Harbour is generally low because the majority of riverine sediments are flushed out to sea.

## 2.2. Wave Climate and Sediment Dynamics

[10] The Bay of Plenty coast is sheltered from New Zealand's westerly and southwesterly winds and waves and has a much milder wave climate compared to the exposed west coast. The wave climate is mainly dominated by northeasterly waves produced by tropical cyclones and from barometric depressions that move down from the northwest and pass through north of New Zealand. Shallow water waves of 0.5–1.5 m wave height and 7–9 s periods dominate the region [Pickrill and Mitchell, 1979; Gorman et al., 2003]. The Bay of Plenty coast is an open sand system exposed to wave

energy and contains the longest littoral drift system of the northeast region. The net littoral drift is around  $70,000 \pm 20,000 \text{ m}^3$  per year and is generally southeasterly directed.

[11] The hydrodynamics at the southern Tauranga Harbour entrance are dominated by tidal currents and waves. Sediment transport is mainly controlled by tidal currents with wave action having a significant effect only in shallow areas. Within the southern port of Tauranga Harbour, the two main tidal channels, Western and Cutter channels (Figure 1a), merge at the southern entrance and are characterized by ebb-directed sediment transport [Kwoll and Winter, 2011]. A conceptual model of sediment dynamics explains that flood tidal currents transport sediment into the inlet, where a sediment circulation pattern develops. Sediment jetted out of the southern Tauranga entrance tends to move landward along the Matakana coast due to wave action.

### 3. Materials and Methods

[12] A sediment sampling survey with research vessel *Tai Rangahau* (University of Waikato, Hamilton, New Zealand) was undertaken during February – March 2010, in the framework of the International Research Training Group INTERCOAST- ‘Integrated Coastal Zone and Shelf Sea Research’ at the Universities of Bremen and Waikato. With an objective to develop the potential of magnetic minerals as markers of coastal zone evolution, a total of 245 surface sediment samples (uppermost 1–5 cm) were collected from the seafloor at water depths from 2.5 to 25 m using a Van Veen grab sampler. Five cross-shore profiles at Waihi Beach (WB), Northern (NM), Central (CM) and Southern (SM) Matakana Island, and Omanu Beach (OB) were sampled at intervals of 50 m in the nearshore region and step-wise increased intervals of 100, 200 and 400 m in the offshore region. Surface sediment samples were also collected along five north–south oriented transects (TH-1, TH-2, TH-3, TH-4 and TH-5) in the southern part of Tauranga Harbour (Figure 1a).

#### 3.1. Environmental Magnetic Analyses

[13] Magnetic measurements were made on dried surface sediment bulk samples. Samples were weighed and densely packed into  $6.2 \text{ cm}^3$  plastic cubes. Magnetic susceptibility was measured at low frequency (0.47 kHz) using a Bartington Instruments MS2B meter. An anhysteretic remanent magnetization (ARM) was imparted in a 100 mT alternating field (AF) and a 40  $\mu\text{T}$  direct current

(DC) bias field using an automated 2G Enterprises 755R DC SQUID pass-through cryogenic magnetometer. An isothermal remanent magnetization (IRM) was imparted and measured at 22 incremental steps up to 700 mT. The IRM at this maximum field was considered as the saturation IRM (SIRM). All results are presented as dry mass specific susceptibilities and remanences.

[14] Raw volume specific magnetic susceptibility values  $\kappa$  were converted to respective mass specific susceptibility  $\chi$  using the calculated density based on known sample mass and volume. Magnetic susceptibility is often used as an indicator for ferromagnetic mineral concentration due to the particle size independence of this parameter [Heider *et al.*, 1996] and because para- and antiferromagnetic minerals generally make a minor magnetic contribution to susceptibility [Thompson and Oldfield, 1986]. Magnetite percentage was calculated considering a value of  $660 \times 10^{-6} \text{ m}^3 \text{ kg}^{-1}$  for pure multidomain magnetite [Maher, 1988]. The ARM/IRM ratio is a common magnetic grain size proxy, which is proportional to the relative content of single domain (SD) particles e.g., for equidimensional magnetite, the (30–100 nm grain size range) and pseudo-single domain (PSD) magnetite (i.e., the 100 nm–1  $\mu\text{m}$  size range) [Muxworthy and Williams, 2006].

#### 3.2. Physical Grain Size and Hydraulic Behavior

[15] Grain size distributions within the 0.4–2000  $\mu\text{m}$  range were measured using a Coulter LS 200 laser particle size analyzer to investigate the influence of particle size on hydraulic behavior and magnetic properties. Suspensions were prepared by placing about 4–5 g of moist sediment into 100 ml of distilled water with addition of 300 mg of a dispersing agent ( $\text{Na}_4\text{P}_2\text{O}_7 \times 10 \text{ H}_2\text{O}$ ) and treated with ultrasonics before measurements were taken. For determination of settling velocities, bulk sediment samples were sieved to remove gravel and clay size particles and were chemically treated to remove organic and carbonate-rich materials [Carver, 1971]. Measurements were performed in an automated settling tube at the Senckenberg Institute for Marine Geology, Wilhelmshaven, Germany.

#### 3.3. Magnetic Grain Size Fractions

[16] Based on bulk magnetic measurements and grain size analyses, four representative samples from each identified unit (beach zone, inner and outer magnetite enrichment belts, offshore zone) were

sieved for 15 min in an automated sieve shaker and separated into the six particle size fractions  $>500 \mu\text{m}$ ,  $355\text{--}500 \mu\text{m}$ ,  $250\text{--}355 \mu\text{m}$ ,  $125\text{--}250 \mu\text{m}$ ,  $63\text{--}125 \mu\text{m}$ , and  $40\text{--}63 \mu\text{m}$ . The particle assemblages obtained in each size fraction were then subjected to the above mentioned magnetic measurements.

### 3.4. Wave Parameters

[17] The cross-shore distribution of physical wave parameters (wave energy, seabed orbital velocity, alongshore wave energy flux) for studying the influence of waves on the bottom sediments were calculated for the open coast sites following equations from Komar [1998] with the influence of breaking in the surf-zone modeled using the method presented by Thornton and Guza [1983]. The model was initialized using wave data over seven years (23 Sept. 2003–02 June 2010) from the Pukehina wave buoy located to the southeast of the study area ( $37.3812^\circ \text{S}$ ,  $176.947^\circ \text{E}$ ) in 62 m water depth. This wave buoy was operated by the Bay of Plenty Regional Council and measured  $H$  (wave height),  $\theta$  (wave direction relative to the orientation of the coast) and  $T$  (wave period).

[18] Based on the Pukehina wave buoy data, the wave energy  $E$  was calculated following Thornton and Guza [1983]:

$$E = \frac{1}{8} \rho g H_{rms}^2, \quad (1)$$

where  $\rho$  is the density of water,  $H_{rms}$  is the root mean square of wave height and  $g$  is the acceleration due to gravity. The alongshore wave energy flux  $S$  was calculated using the identity:

$$S = EC_g \sin(\theta). \quad (2)$$

The cross-shore distribution of wave energy was calculated numerically by solving:

$$\frac{\Delta(C_g E)}{\Delta x} = \langle \varepsilon_b \rangle, \quad (3)$$

where  $C_g$  is the wave group speed, and  $x$  is the cross-shore distance. The wave dissipation due to surfzone breaking  $\langle \varepsilon_b \rangle$  is calculated following Thornton and Guza [1983]:

$$\langle \varepsilon_b \rangle = \frac{3\sqrt{\pi}}{16} g \rho B^3 f \frac{H_{rms}^7}{\gamma^4 h^5}, \quad (4)$$

where  $h$  is the water depth,  $f$  is the cyclic wave frequency,  $\gamma$  is a breaking constant set to 0.42 and  $B$  is a fitting constant set to 1.2 as recommended by

Thornton and Guza [1983]. The seabed orbital velocity  $u$  for intermediate water depth and pure wave motion was calculated using their equation:

$$u = \frac{\pi H}{T} \frac{\cosh(k(h+z))}{\sinh(kh)}, \quad (5)$$

where  $k$  is the radian wave number and  $z$  is the elevation below still water level. The critical velocities  $u_m$  under waves needed to entrain the sediments of fine and medium sands, representing the inner and outer enrichment belts, were calculated following Komar and Miller [1973]:

$$\frac{\rho u_m^2}{(\rho_s - \rho)gD} = a''(d_o/D)^{1/2}, \quad (6)$$

where  $a'' = 0.21$  is the proportionality coefficient calculated based on the average of Bagnold [1946] and Manohar [1955],  $\rho_s$  is the sediment grain density,  $D$  is the sediment grain size and  $d_o$  is the seabed orbital diameter given by:

$$d_o = \frac{H_{rms}}{\sinh(kh)}. \quad (7)$$

The 1D wave transformation model was applied along an average transect for each wave record in the 7-year time series and provided the across-shore distribution of wave characteristics, including the effects of shoaling and wave breaking. The 10%, 50% and 90% probability of occurrence of wave conditions were then calculated from this data set.

### 3.5. Numerical Modeling of Tidal Currents

[19] The estuarine tidal currents were calculated using the 3D hydrodynamic model software “Estuary, Lake and Coastal Ocean Model” (ELCOM), which was earlier set up and calibrated to determine the velocities and direction of tide-induced residual currents within Tauranga Harbour. This model has been previously used to predict velocity, temperature and salinity distribution in natural water bodies [Hodges *et al.*, 2000]. The hydrodynamics simulation method solves the unsteady Reynolds-averaged, hydrostatic Boussinesq, Navier–Stokes and scalar transport equations. Water level conditions along the open ocean boundary of the model domain were derived from the National Institute of Water and Atmospheric Research (NIWA) tidal model (<http://www.niwa.co.nz/our-services/online-services/tides>). The freshwater inflow boundaries into the southern basin of Tauranga Harbour were sourced from Bay of Plenty Regional Council’s monitoring data archives. The bathymetry grid was obtained from hydrographic surveying undertaken by the NZ Navy and

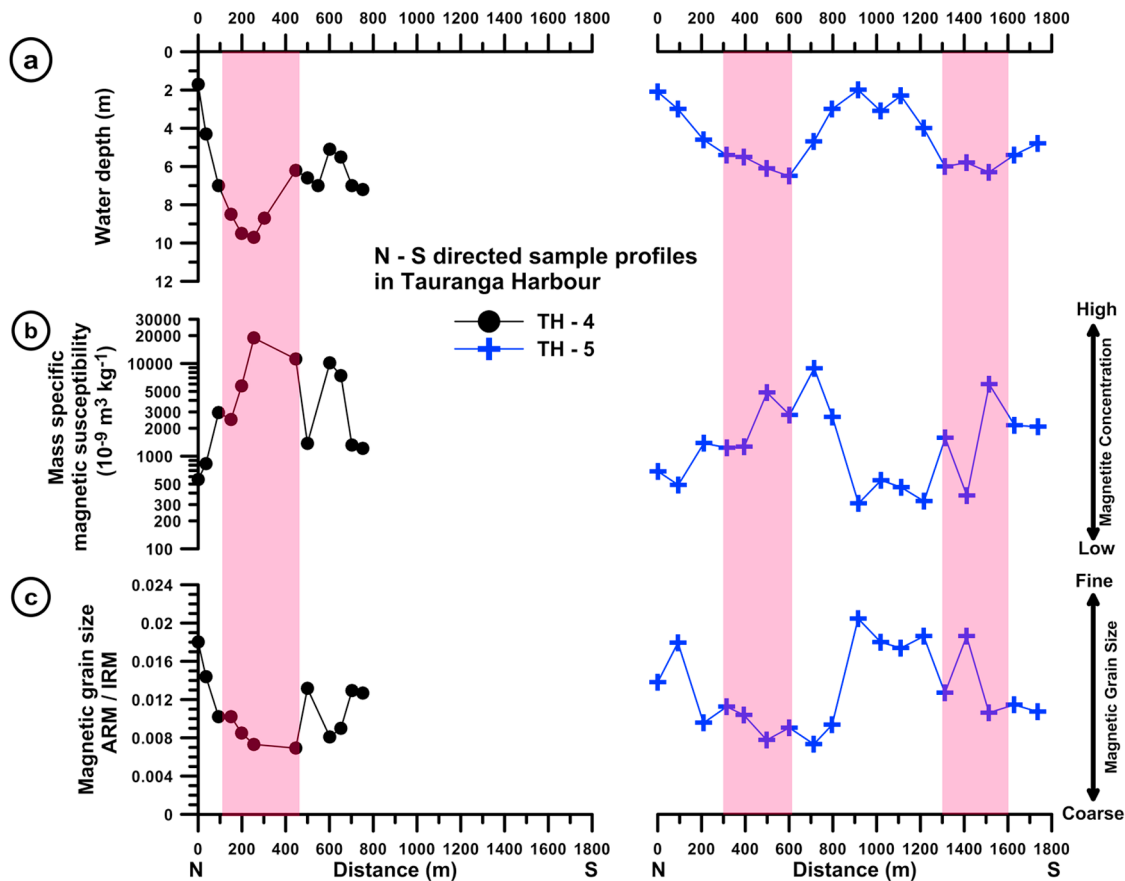


**Figure 2.** Variation of magnetic properties along N–S directed profiles within the southern basin of Tauranga Harbour. The zero on the  $x$  axis marks the north of the sample profiles. (a) Variation in water depth. (b) Mass specific magnetic susceptibility represents the abundance of ferrimagnetic minerals (magnetite), and (c) the ratio of ARM/IRM is used as an indicator of magnetic grain size. Data from profiles TH-4 and TH-5 are shown to illustrate clear trends in magnetic properties compared to all other profiles. Samples from the tidal channel (Western Channel) are highlighted by a pink background. Lower ratios indicate the dominance of coarser magnetic grains, while higher ratios indicate the dominance of finer grains.

the Port of Tauranga. The model was run for a 14-day spring-neap cycle and the output averaged to provide net residual currents.

## 4. Results

### 4.1. Surficial Variation of Magnetite Concentration

[20] Magnetic susceptibility and ARM/IRM data for surficial sediments in and offshore Tauranga Harbour indicate highly variable magnetite concentration and grain size (Figures 1–3). Within the southern basin of Tauranga Harbour, susceptibility varies over two orders of magnitude from 309 to  $18,823 \times 10^{-9} \text{ m}^3 \text{ kg}^{-1}$  ( $\sim 0.05$  to 3 mass % magnetite), with highest values found within tidal channels (Figure 2b). The ARM/IRM ratio for profiles TH-4 and TH-5 varies from 0.006 to 0.020. Higher magnetic susceptibility

values are dominated by coarser magnetic grain sizes and are concentrated in the tidal channels of the southern basin of Tauranga Harbour (Figures 1, 2b, and 2c).

[21] Off Matakana Beach, two coast-parallel belts of magnetite enrichment were identified based on the magnetic susceptibility of five cross-shore profiles (Figure 1). The inner magnetite enrichment belt, which extends from about 800 to 1800 m offshore, appears to connect to the southern entrance (profile SM) and vanishes toward the northern entrance of Tauranga Harbour (profile NM). The outer belt extends from about 2000 to 3500 m from the shoreline and appears to be a larger feature extending toward the north (Figure 1a). The two magnetite enrichments belts are centered in water depths of 6–10 and 10–20 m, respectively (Figure 3b).

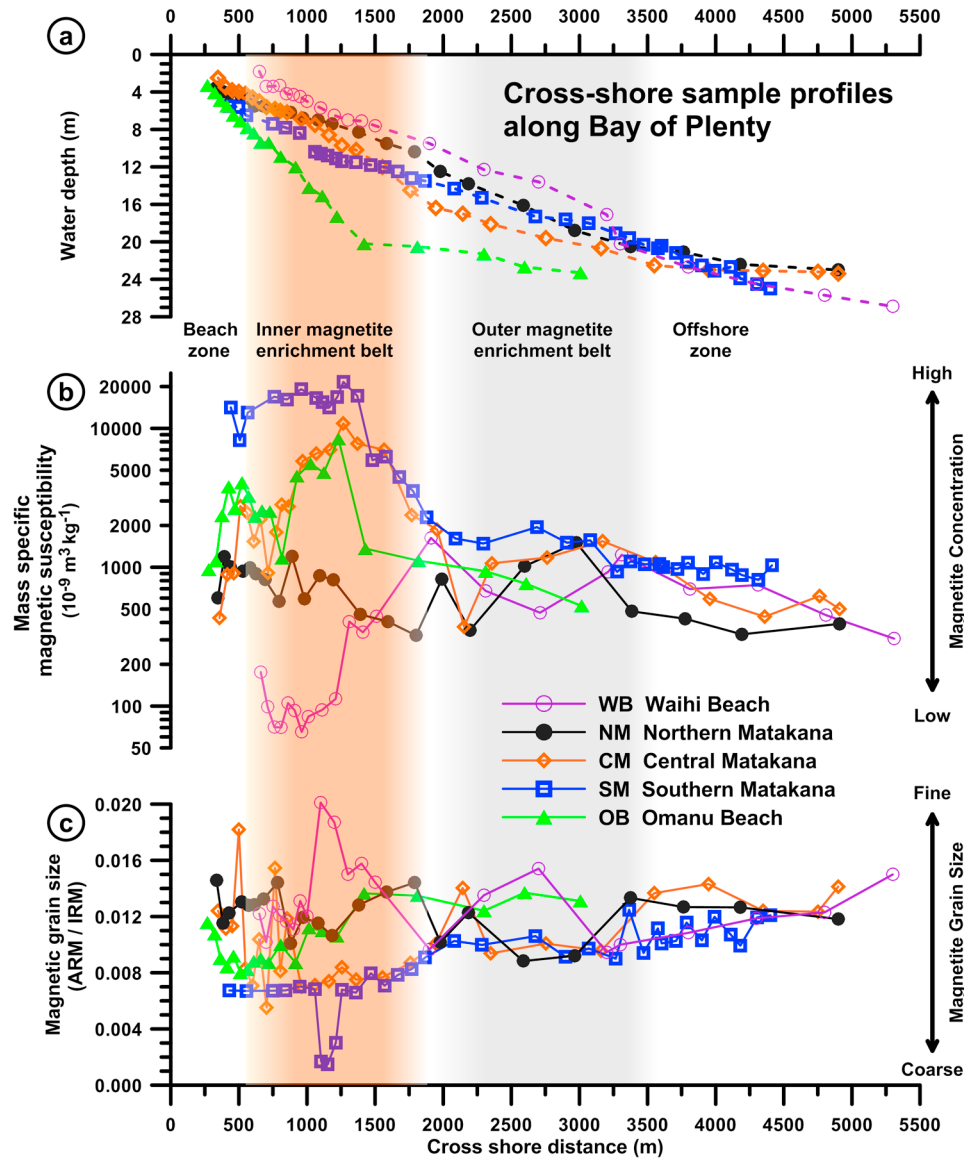


**Figure 3.** Cross-shore variation in (a) water depth, (b) magnetic susceptibility, and (c) magnetic grain size measured on sediment samples from the five offshore profiles shown in Figure 1. Two coast-parallel magnetite enrichment belts are highlighted using color gradients. The inner magnetite enrichment belt is indicated by light brown and the outer belt by gray shading. Lower ARM/IRM ratios indicate the dominance of coarser magnetic grain sizes.

[22] Four different zones were defined by changes in the surficial magnetic susceptibility: the beach zone (water depth 0–6 m), the inner magnetite enrichment belt (6–10 m), the outer magnetite enrichment belt (10–20 m) and an offshore zone (20–25 m) (Figure 3). Overall, the magnetic susceptibility of offshore samples varies over three orders of magnitude from  $65$  to  $21,606 \times 10^{-9} \text{ m}^3 \text{ kg}^{-1}$  ( $\sim 0.01$  to  $3.3$  mass% magnetite) with the highest values within the inner magnetite enrichment belt of profile SM (Figure 3b). The magnetic susceptibility increases from the beach zone to the inner magnetite enrichment belt and then generally decreases with

increasing cross-shore distance. A small susceptibility peak at 2000 to 3500 m offshore marks the outer magnetite enrichment belt (Figure 3b). However, separation between the inner and outer belt is less distinct in profile SM. A general fining trend in magnetite grain size with cross-shore distance is observed in three profiles (CM, SM, OB) as indicated by the increasing ARM/IRM ratio (Figure 3c). In profiles NM and WB, in the beach zone and the inner magnetite enrichment belt the ARM/IRM ratio is relatively high, but it still mirrors the magnetic susceptibility trend.

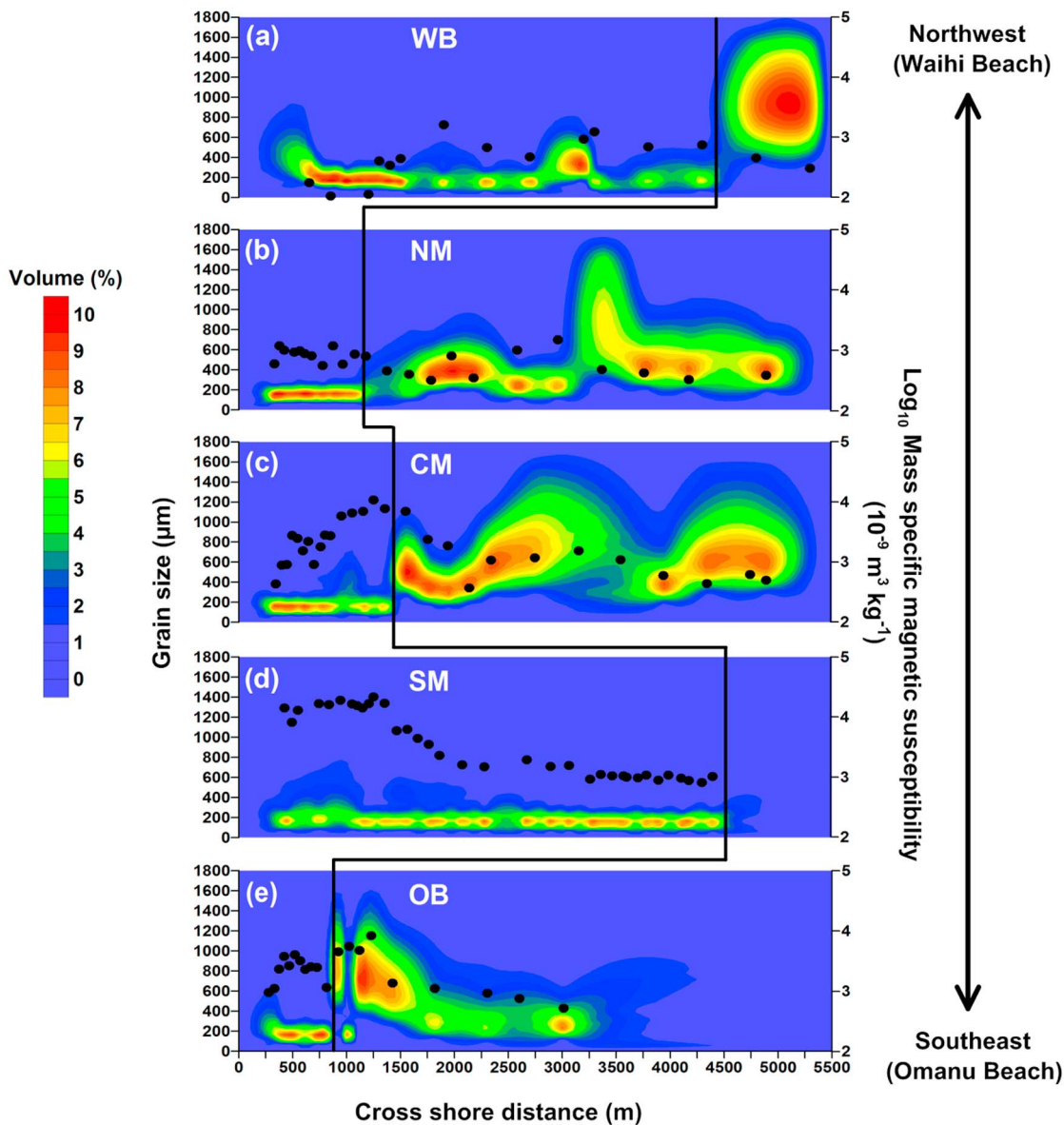


**Figure 4.** Grain size distributions along the five cross-shore profiles. (a) Waihi Beach (WB), (b) Northern Matakana (NM), (c) Central Matakana (CM), (d) Southern Matakana (SM), and (e) Omanu Beach (OB). The vertical scales indicate grain sizes, while those on the right-hand side represent  $\log_{10}$  mass specific magnetic susceptibilities. Solid black circles mark variations in magnetite concentration along the profile as indicated by mass specific magnetic susceptibility values. A solid black line indicates the seaward limit of fine sand along cross-shore profiles.

#### 4.2. Grain Size Distribution Patterns

[23] Grain sizes in and offshore of Tauranga Harbour vary from fine to coarse sand. Well sorted, fine to medium sand dominates the southern basin (data not shown). Offshore of Tauranga Harbour, we observed two different patterns in the cross-shore and along-shore distribution of sediment grain sizes (Figure 4). The nearshore region, including the beach zone and inner magnetite enrichment belt ( $<10$  m water depth), is dominated by fine sand ( $\sim 150$   $\mu\text{m}$ ) and further

coarsens toward the outer belt and offshore zone ( $>10$  m water depth) as observed in profiles NM, CM, and OB (Figures 4b, 4c, and 4e).

#### 4.3. Particle Size Dependent Magnetic Measurements

[24] In highly energetic coastal environments, magnetic properties have a strong dependence on particle size [Oldfield *et al.*, 1985; Yu and Oldfield, 1993;

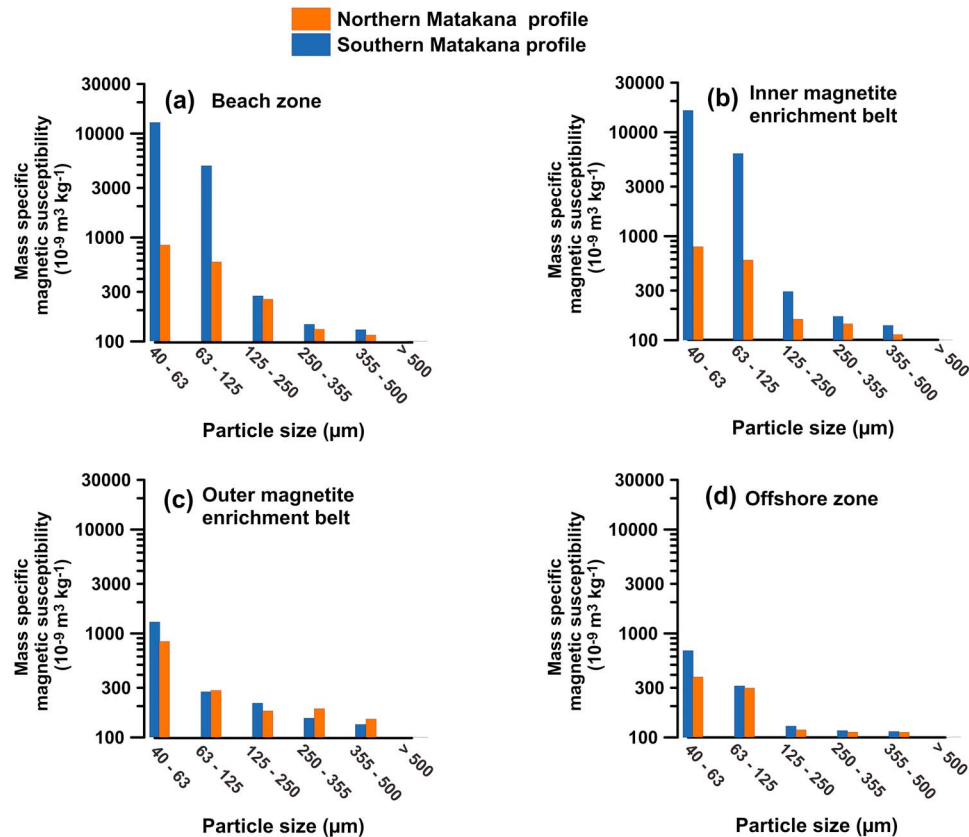


**Figure 5.** Bar plot of cross-shore variations in magnetic mineral concentration for six particle size fractions extracted from bulk sediment samples. The northern and southern Matakana profiles are divided into four different regions: (a) beach zone, (b) inner magnetite enrichment belt, (c) outer magnetite enrichment belt, and (d) offshore zone. Higher susceptibility values correspond to higher magnetite concentrations in each of the sieved fractions.

Hatfield and Maher, 2008]. Measurements of magnetic susceptibility of sieved fractions provide a more detailed understanding of prevailing depositional processes compared to bulk sample measurements. The results of magnetic measurements on different particle size fractions from cross-shore profiles NM and SM are shown in Figure 5. These profiles were chosen because they have the most contrasting differences in magnetic susceptibility and magnetic grain size. Magnetic susceptibility decreases with increasing particle size, with the highest values in the inner magnetite enrichment belt (Figures 5a–5d). For example, in profiles NM and SM, the finer fractions (40–63  $\mu\text{m}$  and 63–125  $\mu\text{m}$ ) generally have a higher magnetic susceptibility than the coarser fractions (>125  $\mu\text{m}$ ) although magnetic susceptibility is variable in the outer belt with much higher values in coarser particle size fractions (125–250  $\mu\text{m}$ , 250–355  $\mu\text{m}$ ; Figure 5c). Overall, the magnetic susceptibility for the SM profile samples is higher and varies over one order of magnitude compared to samples collected from profile NM,

especially in the beach zone and the inner magnetite enrichment belt (Figures 5a and 5b).

#### 4.4. Wave Induced Initiation of Sediment Grain Motion

[25] A mean significant wave height of 0.6 m was calculated in the shallow waters off Tauranga at water depths up to 26 m. Seabed orbital velocities for fair (10%), average (50%), and storm (90%) weather conditions have been calculated based on equation (5) and the wave parameters are given in Table 1. Seabed orbital velocities are high in the beach zone and decrease away from shore (Figure 6a). Critical velocities for the two dominant grain sizes (150 and 400  $\mu\text{m}$ ) that represent the inner and outer magnetite enrichment belt were calculated using equation (6) and are shown as horizontal lines in Figure 6a. The median wave conditions are most likely to suspend the 150  $\mu\text{m}$  grain size fraction in water depths shallower than 10 m. In storm conditions, particles with this grain

**Table 1.** Wave Parameters and Critical Velocities for Two Dominant Grain Sizes

Cross-Shore Distance (m)	Water Depth (m)	Wave Height (m)			Seabed Orbital Velocity (m/s)			Critical Velocity (m/s)	
		10%	50%	90%	10%	50%	90%	150 $\mu\text{m}$	400 $\mu\text{m}$
120	0.5	0.127	0.145	0.152	0.268	0.315	0.331	0.198	0.253
540	5.02	0.281	0.542	1.058	0.140	0.315	0.659	0.202	0.258
1400	10.19	0.277	0.518	1.113	0.053	0.168	0.418	0.178	0.227
2300	15.89	0.280	0.521	1.107	0.015	0.105	0.285	0.163	0.209
3300	20.27	0.285	0.528	1.114	0.005	0.074	0.218	0.155	0.198
4300	23.43	0.289	0.531	1.122	0.002	0.057	0.182	0.148	0.190

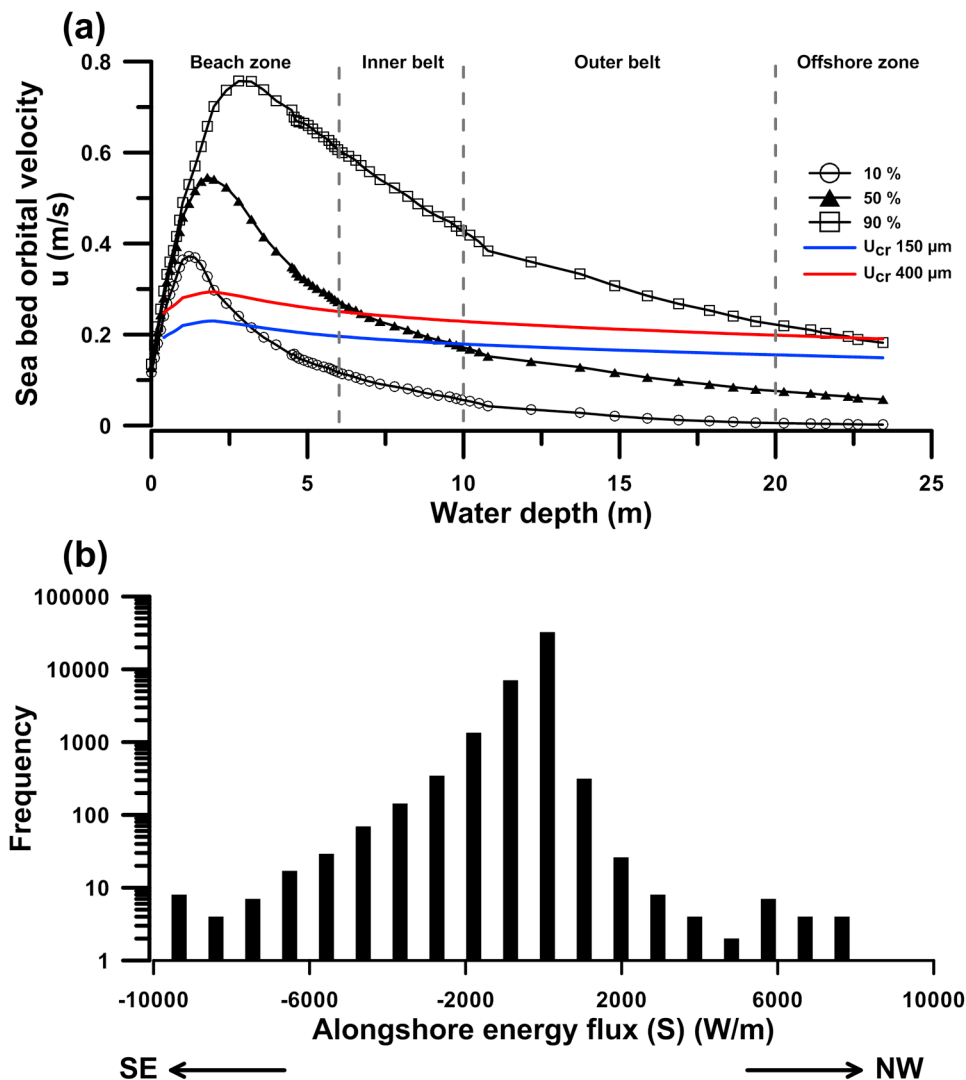


**Figure 6.** Computed wave parameters. (a) Seabed-orbital velocity (calculated using model runs on wave data and equation (5), from which the 10% (fair), 50% (median) and 90% (storm) probabilities were calculated). The horizontal lines marked in blue and red are the critical velocities for the two dominant grain sizes (150  $\mu\text{m}$  and 400  $\mu\text{m}$ ) that were calculated using equations (6) and (7). (b) The probability distribution of alongshore energy flux at the buoy location, calculated using 41655 measurements of wave height and direction data and equations (1) and (2).

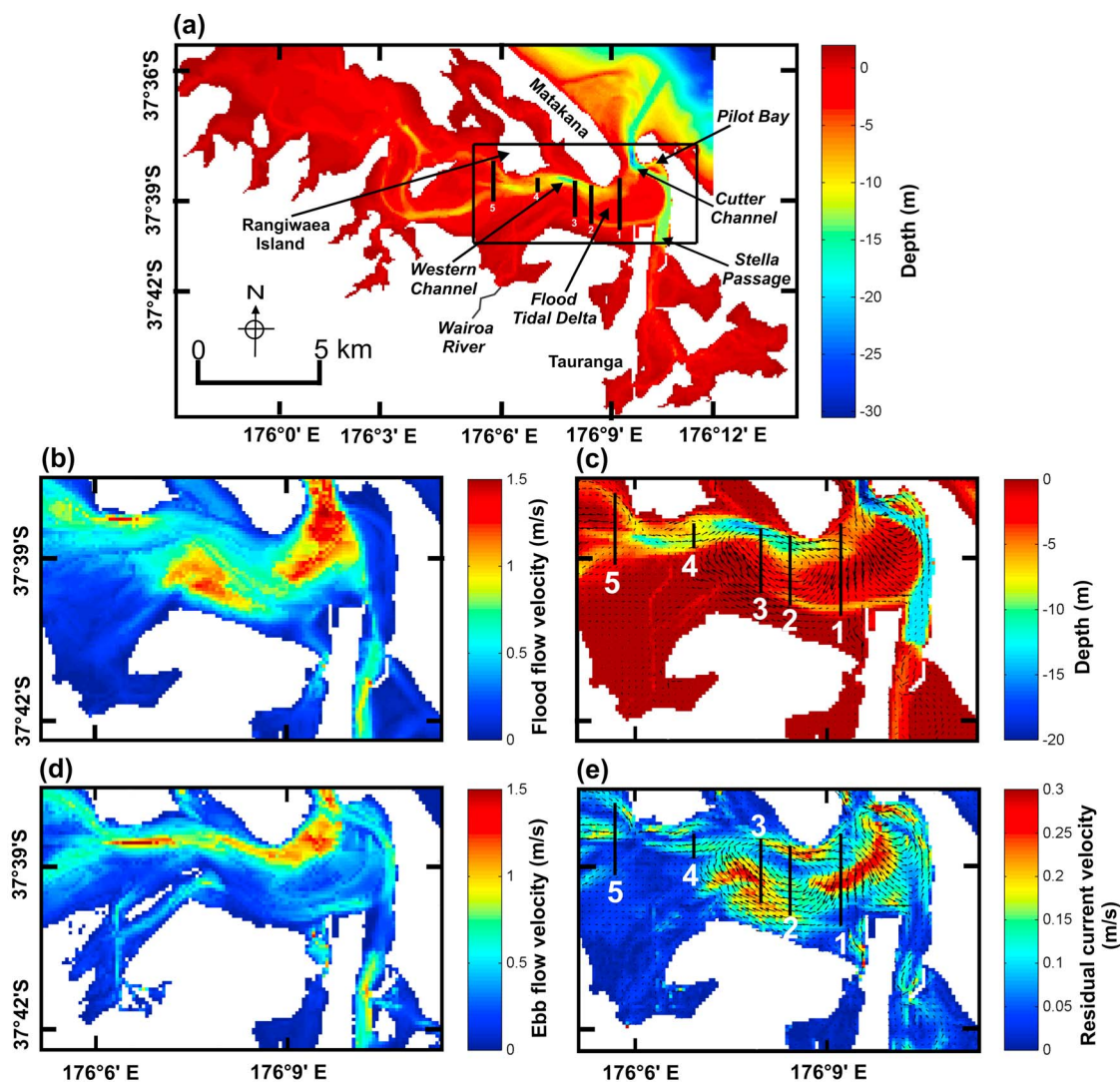


**Figure 7.** (a) Overall bathymetric map of Tauranga Harbour with positions of sediment sampling profiles, (b) modeled peak flood flow velocities ( $\text{ms}^{-1}$ ), (c) time-averaged residual current vectors, (d) peak ebb flow velocities ( $\text{ms}^{-1}$ ), and (e) time-averaged residual current velocities ( $\text{ms}^{-1}$ ). Sediment sampling profiles within Tauranga Harbour are labeled as 1–5. The flood, ebb and residual current velocities are averaged over the entire water column.

size are in continuous motion along the whole profile. Conversely, the coarser grain size fraction ( $400 \mu\text{m}$ ) is suspended only in storm conditions. There are no normal conditions where waves will suspend this size fraction in the offshore zone where it dominates the seabed, which implies that current hydrodynamic conditions are not responsible for deposition of these sediments. The alongshore wave energy flux calculated for the seven years of available wave data indicates that the alongshore transport is bidirectional, but predominantly southeasterly directed (Figure 6b). This indicates that in the region where the grains are suspended by wave processes (shallow region), they will be moved both up and

down the coast, but with a marginal probability that the SE direction will dominate.

#### 4.5. Residual Tidal Currents

[26] Residual vector plots in which the tidal current vector is summed over a spring-neap cycle (14 days) are used to indicate potentially net-driven sediment transport. Peak flood tidal velocities are dominant along the western side of the lagoon entrance and progressively diverge over the shallower central intertidal areas of the flood tidal delta (Figure 7b). Conversely, the peak ebb flow pattern indicates strong currents at the eastern side of the lagoon

entrance and at the Western Channel, while currents are weak over the flood tidal delta (Figure 7d). Time-averaged residual current vectors and velocities within the southern basin of Tauranga Harbour are shown in Figures 7c and 7e. The eastern side of the entrance channel at Pilot Bay, Stella Passage and Western Channel are ebb dominated (Figure 7e), while flood tidal delta and shallower intertidal regions of the upper reaches of Tauranga Harbour are dominated by flood tides. The strength of residual current intensity at Western Channel and the flood tidal delta indicates the importance of tidal asymmetries, ebb and flow dominance, bathymetry and tidal current intensity in driving overall sediment movement within Tauranga Harbour.

#### 4.6. Relationship Between Magnetic Properties and Physical Grain Size

[27] In order to evaluate the relationship between magnetic mineral concentration and physical grain size, bivariate plots are used to indicate magnetic mineral concentration, magnetite grain size and physical grain size (Figure 8). A clear relationship exists between magnetic susceptibility and magnetic grain size in all samples in and offshore of Tauranga Harbour, with highest values dominated by coarser magnetic grain sizes (Figures 8b and 8e). Within the lagoon tidal channel, samples from profiles TH-4 and TH-5 have higher magnetic susceptibilities and coarser physical grain sizes ( $\sim 300\text{--}500\ \mu\text{m}$ ) compared to non-tidal channel samples which have mainly lower magnetic susceptibilities and finer physical grain sizes (Figures 8a and 8c).

[28] Offshore Tauranga Harbour, magnetic susceptibilities are much higher for the inner belt than for the outer belt samples. Inner belt samples from profiles CM, SM and OB have higher susceptibility, coarser magnetic and finer physical grain size compared to outer belt samples; however, this trend is not observed in profile NM and is reversed in profile WB (Figures 8e and 8f). Relevant magnetite enrichments in the Bay of Plenty study area are only observed for fine, mobile ( $\leq 150\ \mu\text{m}$ ) and coarse, non-mobile ( $\geq 600\ \mu\text{m}$ ) sands. Compared to these shelf sediments, samples taken from Tauranga Harbour are generally coarser and lack a fine fraction ( $< 200\ \mu\text{m}$ ; Figures 8a and 8c).

[29] Coupling between magnetic grain size and physical grain size is generally weak for both sample sets (Figures 8a and 8d). Within Tauranga Harbour (Figure 8a), our observations indicate that physical and magnetic grain sizes follow equivalent trends in

response to bottom current conditions. Offshore of Tauranga Harbour (Figure 8d), we observe two populations, where mobile median grain sizes  $< 200\ \mu\text{m}$  have a wide range of magnetite grain sizes that fine with distance from the southern inlet. Immobile sand samples with median grain sizes  $> 200\ \mu\text{m}$  have relatively uniform magnetic grain sizes.

## 5. Discussion

[30] Our results demonstrate the presence, spatial distribution and hydrodynamic drivers of magnetically enriched zones in and around Tauranga Harbour. As verified by electron microscopy (data not shown) and standard mineral magnetic techniques, the magnetic properties are controlled by sedimentary (titano-) magnetite with variable concentration and grain size. We now discuss some of the environmental factors that influence heavy mineral (magnetic and non-magnetic) enrichment processes in estuarine and nearshore regions.

### 5.1. Influence of Sediment Particle Size on Magnetic Properties

[31] Particle size has a decisive influence on certain magnetic properties of sediments [Oldfield and Yu, 1994; Clifton *et al.*, 1999; Zhang *et al.*, 2001]. Magnetic measurements on sieved fractions are often preferred over bulk measurements to discard the generally nonlinear grain size effects. As highlighted by Hounslow and Maher [1996], magnetic minerals, in particular magnetite, often occur as inclusions within silicate minerals such as quartz or feldspar. It is therefore likely that magnetic properties of coarser particle size fractions are partially due to magnetite inclusions in silicate or polycrystalline particles, which decouples magnetic crystal and physical grain size.

[32] In the beach zone and inner magnetite enrichment belt, the fine grain size fractions ( $40\text{--}63\ \mu\text{m}$  and  $63\text{--}125\ \mu\text{m}$ ) have the highest magnetite enhancement, the most prominent alongshore decrease and the largest relative contribution to total magnetic susceptibility (Figures 5a, 5b, and 5d). In the outer magnetite enrichment belt, the magnetite enrichment in the fine fractions is far less prominent and more magnetite occurs in coarser grain size fractions (Figure 5c). In the offshore zone, magnetite contents are generally lower and mainly concentrated in the  $< 125\ \mu\text{m}$  fractions. Grain size distributions offshore of Tauranga Harbour indicate that sediments of the outer belt, i.e., the inner shelf, are dominated

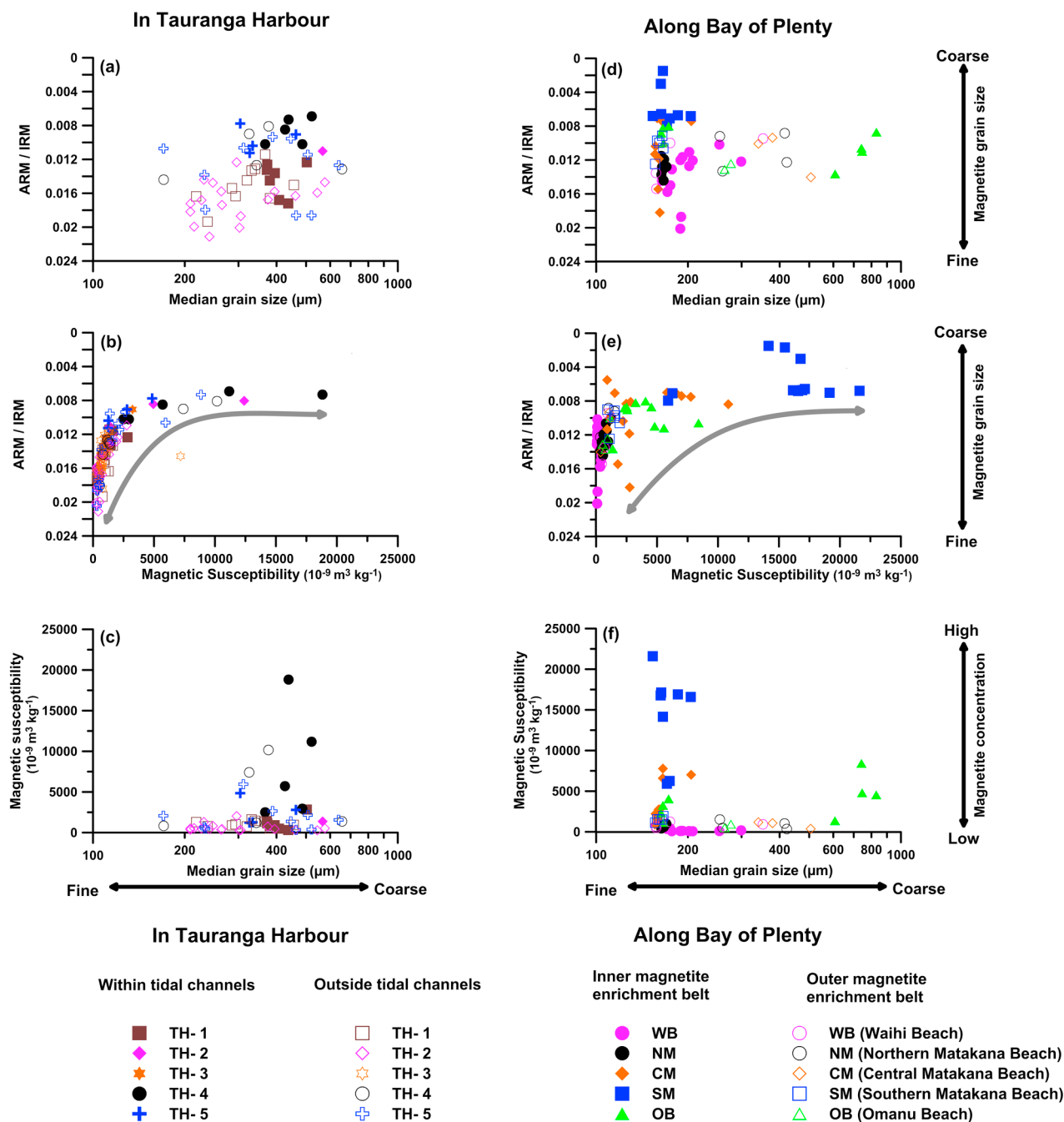


**Figure 8.** Bivariate scatterplots of magnetic grain size (ARM/IRM) versus physical (median) grain size and magnetic susceptibility of surface sediment samples. (a–c) Samples collected within the southern part of Tauranga Harbour. Closed symbols indicate samples from the western tidal channel, and open symbols indicate samples from the non-tidal channel region. (d–f) Samples collected along cross-shore beach profiles along the Bay of Plenty coast covering Waihi, Matakana and Omanu Beach. Closed symbols indicate samples within the inner magnetite enrichment belt, while outer belt samples are marked with open symbols. Note that ordinate scales of Figures 8b and 8e are reversed.

by medium–coarse-grained sand. Previous studies indicate that these sands are relict Pleistocene deposits that were reworked during the last glacial [Harms, 1989; Bradshaw *et al.*, 1994; Michels and Healy, 1999; Krüger and Healy, 2006]. A clear

positive correlation is evident between magnetic susceptibility and magnetic grain size in offshore samples in bivariate plots (Figure 8). This could be a fingerprint for lag deposits and should be further exploited in placer forming environments.

## 5.2. Tide-Induced Residual Currents and Magnetite Enrichment Within Tauranga Harbour

[33] Sediment transport and water circulation in coastal estuaries and lagoons are largely controlled by tides under competing influences of wind stress and river inflow. During flooding, the water depth inside the tidal channels increases and tidal flats are inundated at the peak high tide. These areas are subsequently drained and remain exposed during low tide. These flooding-drying cycles of shallow intertidal flats create or enhance the asymmetry between flood and ebb regimes over a tidal cycle and result in equally asymmetric tidal currents and large-scale residual flows within the lagoon.

[34] Previous studies indicate that sediment dynamics within the southern basin of Tauranga Harbour are mainly dependent on tidal currents. Ebb and flood dominant flows control overall sediment movement within the basin. A residual circulation pattern is developed within the harbor which originates from the lagoon entrance and then moves in a clockwise loop over the flood tidal delta and through the Western Channel before finally returning toward the entrance (Figures 7c and 7e). Sediments from Wairoa River entering the southern basin of Tauranga Harbour are circulated or transported through this residual circulation loop within the harbor.

[35] Residual currents and sediment transport are stronger in Western Channel, Cutter Channel and the flood tidal delta as well as at the lagoon entrance, and are directed toward the inner part of the harbor and contribute to net sediment and water transport within the harbor (Figure 7e). In the upper reaches of Western Channel (Rangiwaia Island), residual currents are smaller, ebb currents are dominant and hence favor sediment deposition by increasing the residence time of mineral grains. As defined by *Dronkers and Zimmerman* [1982], residence time is the period that a water parcel starting from a particular location within a water body remains in the system before exiting. At the lower end of Western Channel and Tauranga Harbour entrance, sediments are flushed more frequently due to stronger tidal action. Profiles TH-4 and TH-5 are located within the upper reaches of the Western Channel and have higher magnetite enrichments in the vicinity of Rangiwaia Island (Figure 7a). This suggests that the smaller ebb-directed residual currents favor higher sediment deposition, and by increasing the residence time of grains, enhance magnetite enrichment within Tauranga Harbour.

[36] There are two related principles for heavy mineral enrichment under strong tidal bottom currents: heavy minerals such as magnetite suspended in hydraulic settling equivalence with larger silicate grains can be less easily entrained from a rough bed after temporary deposition because of their smaller grain size and hence smaller exposure to shear stress compared to lighter minerals. Possibly more importantly, denser minerals at the practically viscous sediment/water interface have negative buoyancy relative to lighter minerals and therefore quickly sink into the deeper, and more protected part of the viscous interface [*Galloway et al.*, 2012]. They are consequently less often remobilized, which over longer terms, results in burial of heavy mineral enriched lag zones. While lighter and smaller particles are continuously lost to the open shelf, heavy mineral enrichments accumulate until they are eventually displaced onto the sublittoral shelf by extreme bottom current velocities such as those associated with spring tides, storm floods or seasonal runoff peaks.

## 5.3. Surf-Zone Processes and Magnetite Enrichment Offshore Tauranga Harbour

[37] Heavy minerals are found enriched on modern beaches, Pleistocene marine terraces, and on the continental shelf. In highly dynamic swash- and surf-zone environments, especially in barrier beaches, placer minerals have been largely concentrated due to reworking of modern and Pleistocene sands. Large amounts of sand in the nearshore region are sorted into heavy mineral enriched lag deposits, while lighter minerals are transported further offshore because of their more frequent remobilization and therefore shorter residence time [*Roy*, 1999].

[38] Our magnetic profile data offshore of Tauranga Harbour reveals the existence of two coast-parallel magnetite enrichment belts in water depths of 6–10 m and 10–20 m. The highest magnetite enrichments were not found in the high-energy beach and breaker zones, but in the calmer nearshore sublittoral zone where sediments consist of well-sorted, fine-grained, mobile Holocene sands. The offshore extension and magnetic enhancement of this facies decreases drastically from E to W. This suggests that this sediment body is not fed by wave action but by coast-parallel transport from Tauranga Harbour's southern entrance. Consequently, the inner magnetite enrichment belt must represent a steady state equilibrium structure, which is progressively dissipated by orbital wave action away from the source. The less prominent, but regionally more uniform,

outer magnetite belt has much lower heavy mineral enrichment, which is comparable to the modern beach facies of the more distal Matakana and Omanu Beach profiles. Owing to immobility of its medium- to coarse-grained sands and its greater lateral continuity, the outer magnetite enrichment belt could therefore represent a late glacial transgressive beach front.

[39] Our findings agree with observations from previous investigations that described two dominant sediment lithofacies (fine and coarse sand) offshore of Tauranga Harbour. These investigations were based on side scan survey and surface sediment sampling campaigns within nearshore and inner shelf areas offshore of Tauranga Harbour [Harms, 1989; Bradshaw *et al.*, 1994; Michels and Healy, 1999; Krüger and Healy, 2006]. These authors showed that coarse-grained sands were partially covered by thin patches and sheets of transgressive fine sands that are transported under low energy conditions, while coarser-grained sands remain in place on the inner shelf as erosional lag or relict deposits.

## 5.4. Influence of Coastal Hydrodynamics and Morphology on Magnetite Enrichment

### 5.4.1. Littoral Drift System and Magnetite Enrichment

[40] The sandy littoral system of Bay of Plenty extends for about 170 km from Waihi Beach in the northwest to Opape in the southeast [Healy, 1980; Hume and Herdendorf, 1990, 1992]. The net littoral drift along Bay of Plenty is generally SE-directed and Waihi Beach is the northernmost end of the littoral drift system [Harray and Healy, 1978; Healy, 1980].

[41] Littoral drift plays a dominant role in along-shore movement of sediments in the nearshore region. Several types of barriers such as headlands, tidal inlets and jetties tend to interrupt the normal littoral drift and cause accumulation of sediments instead of further transport, e.g., near Oregon coast headlands [Peterson *et al.*, 1986]. In our study, this situation corresponds to that of profile SM, which is close to the southern inlet and has the highest concentrations of magnetic minerals. It is possible that the headland at the southern inlet of Tauranga Harbour (Mt. Maunganui) is a potential barrier to the southeasterly directed littoral drift. It disrupts normal delivery of coast parallel sediment flux to the southeast, and causes higher accumulation of finer sediments on the updrift side of the inlet and its ebb-

tidal delta, i.e., along Eastern Matakana Beach. The dredged navigation channel at the southern inlet of Tauranga Harbour also acts as a potential sediment trap for the interrupted littoral drift. Transported offshore by tidal currents, sediments over-spilling from the channel could add to the accumulation of sediment near the southern inlet [Spiers *et al.*, 2009]. However, it is highly unlikely that this alternative W-E offshore enrichment mechanism would gradually lead to a nearly 300-fold increase in magnetite content along the Matakana shore, with nearly the same magnetite enhancement level as an independently acting 60-fold tidal enrichment process of magnetite within the channel network of Tauranga Harbour. We therefore dismiss this explanation for heavy mineral enrichment.

### 5.4.2. Sediment Sorting, Selective Entrainment and Alongshore Sediment Transport

[42] Heavy mineral enrichment in the nearshore region has been well documented in numerous examples around the world [e.g., Komar and Wang, 1984; Bryan *et al.*, 2007]. Accumulation of heavy minerals on the beach and nearshore region produces placer deposits mostly due to gravity separation under the action of waves and currents. For example, in the surf zone, wave breaking results in intense suspension of sediment grains, with fine and heavy grains tending to settle quickly onto the bed whereas lighter and coarser grains are easily entrained and carried away by large waves. Such processes tend to concentrate fine and heavy mineral grains leading to accumulations of fine and dense mineral grains as lag deposits.

[43] Observed resemblances in settling velocities of magnetic and non-magnetic particles within our investigated offshore sediment samples are consistent with the concept of hydraulic equivalence developed by Rubey [1933]. Such similarity in settling velocities is caused by the equivalent and hence reciprocal effect of greater particle density and size, which is commonly observed in placer deposits [Peterson *et al.*, 1986]. This suggests that settling behavior does not play a significant role for heavy mineral enrichment and supports the importance of selective entrainment and burial mechanisms.

[44] Critical velocities calculated for the two dominant grain sizes of the inner and outer magnetite enrichment belts indicate that the finer fraction (<150  $\mu\text{m}$ ) is regularly suspended in water depths less than 10 m which suggests that these sediments are actively involved in beach zone processes (Figure 6a) while the coarser fraction (400  $\mu\text{m}$ ) at

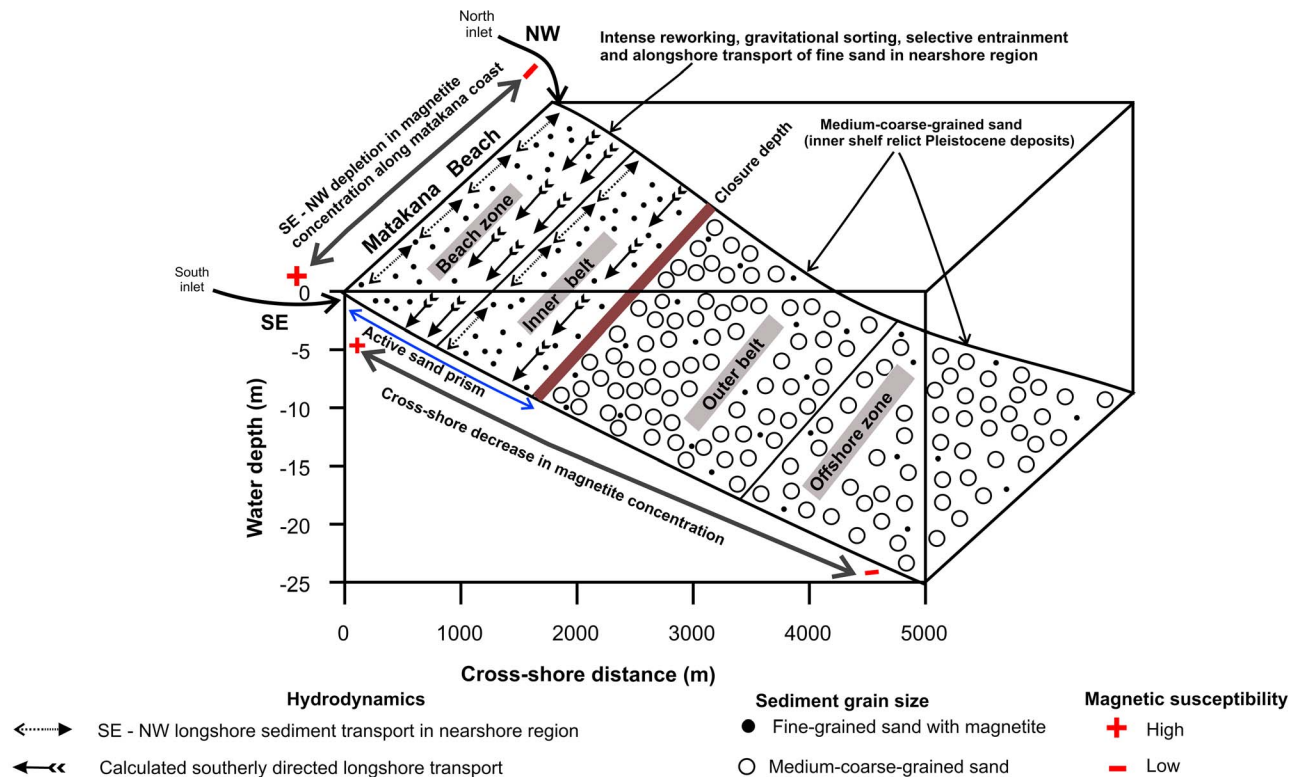


**Figure 9.** Conceptual model for nearshore and inner shelf sediment dynamics off Tauranga Harbour (modified from Bradshaw *et al.* [1994], copyright 1994, with permission from Elsevier).

greater depths of the outer belt and offshore zone remains unsuspected under available energy conditions and form a coarse-grained lag deposit. We therefore hypothesize that the lower boundary of the inner belt (i.e., 10 m water depth) forms the seaward end of the active sand prism or closure depth offshore of Tauranga Harbour, beyond which there is no significant cross-shore or longshore sediment transport. The sharp shift in grain size from fine (150  $\mu\text{m}$ ) to medium (400  $\mu\text{m}$ ) sand is observed in all cross-shore profiles except WB and SM, where sediments are entirely dominated by fine sand (Figures 4a and 4d). An alongshore trend of declining fine sand content is visible in a northwesterly direction between profile SM and NM (Figures 4b–4d). This trend is in accordance with the previously observed decrease in magnetic susceptibility along this profile and indicates a NW-directed alongshore transport of fine sediments in shallow waters.

[45] The alongshore wave energy flux calculation indicates that sediments along Matakana coast generally move southeastward (Figure 6b), but the probability of northwestward movement of sediment

is nearly equivalent. Periodic changes in wave direction and wind pattern provide continuous mixing generated by waves, while more fine-grained sediment is released and suspended at the lagoon entrance forming coast-parallel concentration gradients. Therefore, there will be net drift away from the source (southern inlet) into the northwestern direction, but also into the southeastern direction if the embayments west and east of Mt. Maunganui were interconnected by littoral drift as suggested by consistencies of the Omanu Beach profile. The longshore change in magnetite content and fine sand volume along the Bay of Plenty coast provides evidence for these hypotheses.

## 6. Conclusions

[46] We demonstrate that the combined approach of environmental magnetic, sedimentological and numerical modeling methods is useful to demarcate heavy mineral enriched zones and to delineate their formative processes. Our findings are summarized in a conceptual model (Figure 9), which can probably be generalized to the other offshore

regions. An inner fine-grained heavy mineral belt forms where sediments are diffused away from the lagoonal entrance in the sufficiently energetic nearshore region, while outer enrichment zones are more likely remnants of Pleistocene inner shelf lag deposits. Two key mechanisms that control magnetite enrichment within and offshore of Tauranga Harbour are revealed: tide-induced residual currents control sediment transport within the lagoon and play a key role in forming magnetite-enriched sediment facies. The alongshore distribution of exported and magnetically enriched fine sand is enabled by nearshore wave dynamics and fluctuations in littoral drift, while modern (highstand) surf and swash zone processes yield lower heavy mineral enrichment factors and do not seem to contribute much to the material budget of the inner magnetite enrichment belt. This situation has been different in the past when coastal sands were intensely reworked by rising beachfronts.

[47] Magnetic susceptibility is a useful and easily determined parameter, which efficiently identifies heavy-mineral-rich areas in coastal settings. Heavy minerals represent key indicators of the sedimentary regimes and energy conditions of coastal environments. Determination of magnetic susceptibility of the seafloor by sediment sampling or future electromagnetic profiling has considerable potential to be used as routine tool for coastal and shelf placer mineral exploration.

## Acknowledgments

[48] We acknowledge funding by the Deutsche Forschungsgemeinschaft DFG via the Bremen-Waikato International Research Training Group INTERCOAST and the MARUM Center for Marine Environmental Sciences at the University of Bremen. Liane Brück, Dirk Immenga, Christopher Daly, Serena Fraccascia, Ruggero Capperucci, Max Kluger, Gerhard Bartzke and Sebastien Boulay provided assistance during sampling and Hui Woon Tay provided valuable numerical hydrodynamic modeling results. We are grateful to Terry Healy, Burghard Flemming, Christian Winter and Willem de Lange for their support and helpful inputs. The Bay of Plenty Regional Council, Tauranga, New Zealand is thanked for contributing long-term wave data. Alexander Bartholomä gave access to the automated settling tube facility at the Senckenberg Institute for Marine Geology, Wilhelmshaven, Germany. The Hanse Wissenschaftskolleg, Germany, supported KRB during her study leave at the University of Bremen. The authors thank Stefanie Brachfeld and an anonymous reviewer for detailed and helpful reviews of the manuscript.

## References

- Bagnold, R. A. (1946), Motion of waves in shallow water. Interaction between waves and sand bottoms, *Proc. R. Soc. London, Ser. A*, *187*, 1–18, doi:10.1098/rspa.1946.0062.
- Beanland, S., and K. R. Berryman (1992), Holocene coastal evolution in a continental rift setting; Bay of Plenty, New Zealand, *Quat. Int.*, *15–16*, 151–158, doi:10.1016/1040-6182(92)90043-2.
- Bradshaw, B. E., T. R. Healy, C. S. Nelson, P. M. Dell, and W. P. De Lange (1994), Holocene sediment lithofacies and dispersal systems on a storm-dominated, back-arc shelf margin: The east Coromandel coast, New Zealand, *Mar. Geol.*, *119*, 75–98, doi:10.1016/0025-3227(94)90142-2.
- Bryan, K. R., A. Robinson, and R. M. Briggs (2007), Spatial and temporal variability of titanomagnetite placer deposits on predominantly black sand beach, *Mar. Geol.*, *236*, 45–59, doi:10.1016/j.margeo.2006.09.023.
- Carter, L. (1980), Iron sand in continental shelf sediments of western New Zealand—A synopsis, *N. Z. J. Geol. Geophys.*, *23*, 455–468, doi:10.1080/00288306.1980.10424116.
- Carver, R. E. (1971), *Procedures in Sedimentary Petrology*, John Wiley, New York.
- Cioppa, M. T., N. J. Porter, A. S. Trenhaile, B. Igbokwe, and J. Vickers (2010), Beach sediment magnetism and sources: Lake Erie, Ontario, Canada, *J. Great Lakes Res.*, *36*, 674–685, doi:10.1016/j.jglr.2010.07.007.
- Clifton, J., P. McDonald, A. Plater, and F. Oldfield (1999), Derivation of a grain-size proxy to aid the modelling and prediction of radionuclide activity in salt marshes and mud flats of the eastern Irish Sea, *Estuarine Coastal Shelf Sci.*, *48*, 511–518, doi:10.1006/ecss.1998.0461.
- De Lange, W. P. (1991), Wave climate for No 1 Reach, Port of Tauranga, Tauranga Harbour, report, Port of Tauranga Ltd., Hamilton, New Zealand.
- Dronkers, J., and J. T. F. Zimmerman (1982), Some principles of mixing in tidal lagoons, *Oceanol. Acta*, *4*, 8–14.
- Foster, I. D. L., A. J. Albon, K. M. Bardell, J. L. Fletcher, T. C. Jardine, R. J. Mothers, M. A. Pritchard, and S. E. Turner (1991), High energy coastal sedimentary deposits: An evaluation of depositional processes in southwest England, *Earth Surf. Processes Landforms*, *16*, 341–356, doi:10.1002/esp.3290160407.
- Frihy, O. E., and K. M. Dewidar (2003), Patterns of erosion/sedimentation, heavy mineral concentration and grain size to interpret boundaries of littoral sub cells of the Nile delta, Egypt, *Mar. Geol.*, *199*, 27–43, doi:10.1016/S0025-3227(03)00145-2.
- Galloway, E., A. S. Trenhaile, M. T. Cioppa, and R. G. Hatfield (2012), Magnetic mineral transport and sorting in the swash-zone: Northern Lake Erie, Canada, *Sedimentology*, doi:10.1111/j.1365-3091.2012.01323.x, in press.
- Gorman, R. M., K. R. Bryan, and A. K. Laing (2003), Wave hindcast for the New Zealand region: Nearshore validation and coastal wave climate, *N. Z. J. Mar. Freshwater Res.*, *37*(3), 567–588, doi:10.1080/00288330.2003.9517190.
- Gow, A. G. (1967), Petrographic studies of iron sands and associated sediment near Hawera, South Taranaki, *N. Z. J. Geol. Geophys.*, *10*, 675–696, doi:10.1080/00288306.1967.10431086.
- Hamill, P. F., and P. F. Ballance (1985), Heavy mineral rich beach sands of the Waitakere coast, Auckland, *N. Z. J.*



- Geol. Geophys.*, 28, 503–511, doi:10.1080/00288306.1985.10421203.
- Harms, C. (1989), Dredge spoil dispersion from an inner shelf dump mound, M.Phil. thesis, Dep. of Earth and Ocean Sci., Univ. of Waikato, Hamilton, New Zealand.
- Harray, K. G., and T. R. Healy (1978), Beach erosion at Waihi Beach Bay of Plenty, New Zealand, *N. Z. J. Mar. Freshwater Res.*, 12, 99–107, doi:10.1080/00288330.1978.9515731.
- Hatfield, R. G., and B. A. Maher (2008), Suspended sediment characterization and tracing using a magnetic fingerprinting technique: Bassenthwaite Lake, Cumbria, UK, *Holocene*, 18, 105–115, doi:10.1177/0959683607085600.
- Hatfield, R. G., and B. A. Maher (2009), Holocene sediment dynamics in an upland temperate lake catchment: Climatic and land-use impacts in the English Lake District, *Holocene*, 19, 427–438, doi:10.1177/0959683608101392.
- Hatfield, R. G., M. T. Cioppa, and A. S. Trenhaile (2010), Sediment sorting and beach erosion along a coastal foreland: Magnetic measurements in Point Pelee National Park, Ontario, Canada, *Sediment. Geol.*, 231, 63–73, doi:10.1016/j.sedgeo.2010.09.007.
- Healy, T. R. (1980), Erosion and sediment drift on the Bay of Plenty coast, *Soil Water*, 16, 12–14.
- Heider, F., A. Zitzelsberger, and K. Fabian (1996), Magnetic susceptibility and remanent coercive force in grown magnetite crystals from 0.1  $\mu\text{m}$  to 6 mm, *Phys. Earth Planet. Inter.*, 93, 239–256, doi:10.1016/0031-9201(95)03071-9.
- Hodges, B. R., J. Imberger, A. Saggio, and K. B. Winters (2000), Modelling basin scale waves in a stratified lake, *Limnol. Oceanogr.*, 45, 1603–1620, doi:10.4319/lo.2000.45.7.1603.
- Hounslow, M. W., and B. A. Maher (1996), Quantitative extraction and analysis of carriers of magnetization in sediments, *Geophys. J. Int.*, 124, 57–74, doi:10.1111/j.1365-246X.1996.tb06352.x.
- Hume, T. M., and C. E. Herdendorf (1990), Morphological and hydrological characteristics of tidal inlets on a headland dominated, low littoral drift coast, northeastern New Zealand, *J. Coastal Res.*, 9, 527–563.
- Hume, T. M., and C. E. Herdendorf (1992), Factors controlling tidal inlet characteristics on low drift coasts, *J. Coastal Res.*, 8, 355–375.
- Kear, D. (1979), Geology of iron resources of New Zealand, 164 pp., N. Z. Dep. of Sci. and Ind. Res., Wellington.
- Komar, P. D. (1998), *Beach Processes and Sedimentation*, 2nd ed., Prentice Hall, Upper Saddle River, N. J.
- Komar, P. D., and M. C. Miller (1973), The threshold of sediment movement under oscillatory water waves, *J. Sediment. Petrol.*, 43, 1101–1110, doi:10.1306/74D7290A-2B21-11D7-8648000102C1865D.
- Komar, P. D., and C. Wang (1984), Processes of selective grain transport and the formation of placers on beaches, *J. Geol.*, 92, 637–655, doi:10.1086/628903.
- Krüger, J., and T. R. Healy (2006), Mapping the morphology of dredged ebb tidal delta, Tauranga Harbour, New Zealand, *J. Coastal Res.*, 22, 720–727, doi:10.2112/03-0117.1.
- Kwoll, E., and C. Winter (2011), Determination of initial grain size distribution in a tidal inlet by means of numerical modelling, *J. Coastal Res.*, 64, 1081–1085.
- Lees, J. A., and J. S. Pethick (1995), Problems associated with quantitative magnetic sourcing of sediments of the Scarborough to Mablethorpe coast, northeast England, U.K., *Earth Surf. Processes Landforms*, 20, 795–806, doi:10.1002/esp.3290200905.
- Li, M. Z., and P. D. Komar (1992), Longshore grain sorting and beach placer formation adjacent to the Columbia River, *J. Sediment. Petrol.*, 62, 429–441, doi:10.1306/D426791A-2B26-11D7-8648000102C1865D.
- Maher, B. A. (1988), Magnetic properties of some synthetic sub-micron magnetites, *Geophys. J.*, 94, 83–96, doi:10.1111/j.1365-246X.1988.tb03429.x.
- Maher, B. A., R. Thompson, and M. W. Hounslow (1999), *Introduction to Quaternary Climates, Environments and Magnetism*, Cambridge Univ. Press, Cambridge, U. K., doi:10.1017/CBO9780511535635.
- Manohar, M. (1955), Mechanics of bottom sediment movement due to wave action, *Tech. Memo.*, 75, Beach Erosion Board, U.S. Army Corps of Eng., Washington, D. C.
- Michels, K. H., and T. R. Healy (1999), Evaluation of an inner shelf site off Tauranga Harbour, New Zealand, for disposal of muddy-sandy dredged sediments, *J. Coastal Res.*, 15, 830–838.
- Müller, H., T. von Dobeneck, W. Nehmiz, and K. Hamer (2011), Near-surface electromagnetic, rock magnetic, and geochemical fingerprinting of submarine freshwater seepage at Eckernförde Bay (SW Baltic Sea), *Geo Mar. Lett.*, 31, 123–140, doi:10.1007/s00367-010-0220-0.
- Müller, H., T. von Dobeneck, C. Hilgenfeldt, B. SanFillipo, D. Rey, and B. Rubio (2012), Mapping the magnetic susceptibility and electric conductivity of marine surficial sediments by benthic EM profiling, *Geophysics*, 77, E43–E56, doi:10.1190/geo2010-0129.1.
- Muxworthy, A. R., and W. Williams (2006), Low-temperature viscous magnetization of multidomain magnetite: Evidence for disaccommodation contribution, *J. Magn. Magn. Mater.*, 307, 113–119, doi:10.1016/j.jmmm.2006.03.052.
- Oldfield, F., and L. Yu (1994), The influence of particle size variations on the magnetic properties of sediments from the north-eastern Irish Sea, *Sedimentology*, 41, 1093–1108, doi:10.1111/j.1365-3091.1994.tb01443.x.
- Oldfield, F., B. A. Maher, J. Donoghue, and J. Pierce (1985), Particle-size related, mineral magnetic source sediment linkages in the Rhode River catchment, Maryland, USA, *J. Geol. Soc.*, 142, 1035–1046, doi:10.1144/gsjgs.142.6.1035.
- Peterson, C. D., P. D. Komar, and K. F. Scheidegger (1986), Distribution, geometry, and origin of heavy mineral placer deposits on Oregon beaches, *J. Sediment. Res.*, 56, 67–77, doi:10.1306/212f8887-2b24-11d7-8648000102c1865d.
- Pickrill, R. A., and J. S. Mitchell (1979), Ocean wave characteristics around New Zealand, *N. Z. J. Geol. Geophys.*, 13, 501–520, doi:10.1080/00288330.1979.9515827.
- Rao, C. B. (1957), Beach erosion and concentration of heavy mineral sands, *J. Sediment. Res.*, 27, 143–147, doi:10.1306/74D70682-2B21-11D7-8648000102C1865D.
- Razjigaeva, N. G., and V. V. Naumova (1992), Trace element composition of detrital magnetite from coastal sediments of northwestern Japan Sea for provenance study, *J. Sediment. Res.*, 62, 802–809, doi:10.1306/d42679e2-2b26-11d7-8648000102c1865d.
- Roy, P. S. (1999), Heavy mineral beach placers in southeastern Australia: Their nature and genesis, *Econ. Geol.*, 94, 567–588, doi:10.2113/gsecongeo.94.4.567.
- Rubey, W. W. (1933), The size distribution of heavy minerals within a water laid sandstone, *J. Sediment. Petrol.*, 3, 3–29, doi:10.1306/D4268E37-2B26-11D7-8648000102C1865D.
- Shepherd, M. J., and P. A. Hesp (2003), Sandy barriers and coastal dunes, in *The New Zealand Coast: Te Tai Aotearoa*,



- edited by J. R. Goff, S. L. Nichol, and H. L. Rouse, pp. 163–189, Dunmore, Palmerston North, New Zealand.
- Shepherd, M. J., B. G. McFadgen, and D. G. Sutton (2000), Geomorphological evidence for a Pleistocene barrier at Matakana Island, Bay of Plenty, New Zealand, *N. Z. J. Geol. Geophys.*, *43*, 579–586, doi:10.1080/00288306.2000.9514910.
- Slingerland, R. L. (1977), The effects of entrainment on the hydraulic equivalence relationships of light and heavy minerals in sands, *J. Sediment. Res.*, *47*, 753–770, doi:10.1306/212f7243-2b24-11d7-8648000102c1865d.
- Spiers, K., T. R. Healy, and C. Winter (2009), Ebb-jet dynamics and transient eddy formation at Tauranga Harbour: Implications for entrance channel shoaling, *J. Coastal Res.*, *25*, 234–247, doi:10.2112/07-0947.1.
- Thompson, R., and F. Oldfield (1986), *Environmental Magnetism*, 227 pp., Allen and Unwin, London, doi:10.1007/978-94-011-8036-8.
- Thornton, E. B., and R. T. Guza (1983), Transformation of wave height distribution, *J. Geophys. Res.*, *88*, 5925–5938, doi:10.1029/JC088iC10p05925.
- Wheeler, A. J., F. Oldfield, and J. D. Orford (1999), Depositional and post-depositional controls on magnetic signals from salt marshes on the north-west coast of Ireland, *Sedimentology*, *46*, 545–558, doi:10.1046/j.1365-3091.1999.00236.x.
- Yu, L., and F. Oldfield (1993), Quantitative sediment source ascription using magnetic measurements in a reservoir-catchment system near Nijar, S.E. Spain, *Earth Surf. Processes Landforms*, *18*, 441–454, doi:10.1002/esp.3290180506.
- Zhang, S., M. T. Cioppa, and S. Zhang (2010), Spatial variation in particle size and magnetite concentration on Cedar Beach: Implications for grain sorting processes, western Lake Erie, Canada, *Dizhi Xuebao*, *84*, 1520–1532, doi:10.1111/j.1755-6724.2010.00345.x.
- Zhang, W., L. Yu, and S. M. Hutchinson (2001), Diagenesis of magnetic minerals in the intertidal sediments of the Yangtze Estuary, China, and its environmental significance, *Sci. Total Environ.*, *266*, 169–175, doi:10.1016/S0048-9697(00)00735-X.
- Zimmerman, J. T. F. (1981), Dynamics, diffusion and geomorphological significance of tidal residual eddies, *Nature*, *290*, 549–555, doi:10.1038/290549a0.